A fast generic millimetre-wave emissivity model

Stephen J. English[a] and Tim J. Hewison[b]

[a]Meteorological Office, NWP Division, London Road, Bracknell, Berkshire, RG12 2SZ, UK.
[b]Meteorological Office, Remote Sensing, Building Y70, DERA Farnborough, GU14 6TD, UK.

ABSTRACT

In recent years an increasingly diverse range of passive microwave satellite data has become available for applications in numerical weather forecasting, climate studies and environmental monitoring. Top of atmosphere radiance is measured, which has originated from both the surface and the atmosphere. When retrieving atmospheric quantities such as temperature, humidity or cloud liquid water content near the surface it is necessary to account correctly for the contribution to the measured radiance from the surface. This depends on the surface emissivity, which varies widely with surface type, roughness and temperature. For real time applications such as numerical weather forecasting, it is necessary to be able to model the surface emissivity very quickly. There is therefore a need for a fast surface emissivity model for any surface type, instrument geometry and observation wavelength. A fast generic emissivity model has therefore been developed. This is a semi-empirical model. Some aspects are physically based, for example many surfaces can be assumed to be dielectric media. Other aspects such as geometric roughness have been parameterised for speed. For some complex or poorly understood aspects of the electromagnetic interaction empirical adjustments are made to fit observed values. The model has been compared with emissivities derived from aircraft radiometer measurements at 24, 50, 89 and 157 GHz. It is also intended to compare with data from the Special Sensor Microwave Imager and Advanced Microwave Sounding Unit instruments. For the ocean surface the fast model fits estimated emissivities from airborne radiometers to within 1-2%, and it fits the unparameterised model to within 0.1-0.3%.

Key-words: microwave, millimere-wave, emissivity, AMSU, SSM/I, TRMM, radiometer, radiance, fast-model, ocean, land

1. INTRODUCTION

Radiances measured at the top of the atmosphere now form a key part of the global meteorological observation network for numerical weather prediction (NWP)[1,2,3]. Over the sea passive microwave data have been used for ocean and atmosphere applications, whereas over land and ice surfaces the most extensive studies have been for surface applications. A few studies have attempted to retrieve cloud liquid water over land surfaces[4,5,6,7] and this has recently been extended[8] to the retrieval of skin temperature, water vapour and liquid water using a climatology of emissivity[9]. Humidity retrievals from the Advanced Microwave Sounding Unit are particularly sensitive to emissivity and emissivity model error[10], whereas temperature retrievals are more sensitive to the quality of prior knowledge of skin temperature. These studies have shown that there is potential for retrieving information on cloud liquid water path, temperature and water vapour profiles and skin temperature over land using microwave radiances, but that the information is very sensitive to a range of parameters, including emissivity. With an increasing number of different microwave sensors, and the desire to expand the use of radiance observations over land and ice surfaces, a need has arisen for a generic all-surface emissivity model.

Land surface emissivity has been estimated[9,11,12,13] at high frequency in the context of extending atmospheric parameter retrievals to land and ice surface and recent measurements[15,16,17] have improved estimation of land and ice emissivity at frequencies higher than those used for land and ice surface applications. Theoretical models have primarily been applied using low frequency approximations (e.g. dense medium or strong fluctuation theory) which make them unsuitable for higher frequency applications[18].

This paper presents a generic emissivity model which adopts a semi-empirical approach. At the heart of the model are equations which represent real physical processes, such as specular reflection by a surface, Bragg scattering and layering. However the coefficients used in these models are not physically derived but are based on a mixture of laboratory

measurements and aircraft radiance observations. Although the equations relate to physics which may be inappropriate for some surfaces, it still provides a suitable mathematical framework for a purely empirical model.

2. THE SURFACE EMISSIVITY MODEL

Surfaces can be divided into those which behave like a dielectric medium and those which do not. The former are characterised by homogeneity on a scale large compared to the wavelength of observation. In this case emissivity can be easily calculated if the dielectric properties of the medium are known. If however there are irregularities the theory may have to be modified. It may be possible to treat a heterogeneous medium as an effective dielectric medium with effective dielectric properties[19]. As the complexity of the electromagnetic interaction with the surface increases, more terms need to be added to the estimation of surface emissivity. Where we have no *a priori* information to use in these models, their increased complexity may be of little value for sounding applications. Here the requirement is for a simple model which constrains the retrieval of emissivity in a physical way. One such model has been proposed[20], but this does not predict polarisation or view angle dependence. We extend this approach by bringing it closer to the physical processes which determine the emissivity. There are five components to the model.

2.1 Specular reflection

The Fresnel reflectivities $R_h(\nu,\theta)$ and $R_v(\nu,\theta)$, where ν is frequency of the observed radiance and θ is the incidence angle, can be calculated if the permittivity of the surface is known. For water the permittivity is calculated from laboratory measurements[21] of the Debye parameters. For non-ocean surfaces, an estimation of the Debye parameters is made which gives the best fit to the observed spectral radiance variation, which is measured using airborne radiometers at 24-157 GHz. For surfaces which are not homogeneous (i.e. they do not have a single permittivity) the permittivity is better defined as an effective (rather than average) permittivity i.e. the permittivity which when used in the Fresnel reflection equation gives the observed reflectivities. The Fresnel reflectivities can be written

$$R_v(\nu,\theta) = \left| \frac{-\varepsilon(\nu)\cos(\theta) + \sqrt{\varepsilon(\nu) - \sin^2(\theta)}}{\varepsilon(\nu)\cos(\theta) + \sqrt{\varepsilon(\nu) - \sin^2(\theta)}} \right|^2,$$

$$R_h(\nu,\theta) = \left| \frac{-\cos(\theta) + \sqrt{\varepsilon(\nu) - \sin^2(\theta)}}{\cos(\theta) + \sqrt{\varepsilon(\nu) - \sin^2(\theta)}} \right|^2. \quad (1)$$

The effective permittivity, $\varepsilon(\nu)$, can be calculated from a form of the Debye equation written for n relaxation frequencies as

$$\varepsilon(\nu) = \varepsilon_\infty + \sum_{i=1}^{n} \frac{\Delta_i}{1 - i\nu / \nu_i^r}, \quad (2)$$

$$\sum_{i=1}^{n} \Delta_i = \varepsilon_s - \varepsilon_\infty. \quad (3)$$

For most surfaces only one relaxation frequency (i.e. n=1) is required, so three parameters (ε_s or Δ_1, ε_∞, and ν_1^r) are needed to calculate $\varepsilon(\nu)$, where ε_s is static permittivity and ε_∞ is permittivity at infinite frequency. Ionic conductivity is neglected, because its effect is usually negligible above 20 GHz. For some surfaces the Debye parameters are well defined measurable quantities, e.g. for saline water, where n=2 and Δ_1, Δ_2, ν_1^r, ν_2^r and ε_∞ are functions of SST[21]. For other surfaces they may have no physical meaning but are useful to give form to the parameterisation. This has been applied[16, 17] to land and ice surfaces, deriving the coefficients empirically from measured brightness temperatures over field sites. Because all surfaces other than sea are assumed to have n=1, coefficients are generated for ε_s, ε_∞ and ν_1^r.

2.2 Bragg scattering

It has been shown that Bragg scattering is an important process in determining the surface reflectivity[22,23]. The Fresnel reflectivities are multiplied by a factor $B(\nu,\theta,h)$, where h is a function of small-scale roughness and is again empirically derived from aircraft measurements[16,17]. $B(\nu,\theta,h)$ can be written as,

$$B(\nu,\theta,h) = e^{-h\cos^2(\theta)} \tag{4}$$

where $h=(4\pi\nu\sigma/c)^2$, σ is small scale surface roughness and c is the speed of light. For the ocean it is difficult to separate the small-scale and large scale roughness, to determine σ^2, and various wave-spectra models exist. It has been shown[24] that slope variance has a power-law behaviour of the form k^{-4}, where k is wavenumber across a wide range of wavenumbers. The dependence on windspeed is expected to be close to linear. So it is assumed that σ^2 has the form U^β/ν^4, where U is windspeed and β a constant. Therefore for ocean h is assumed to have the form $\alpha U^\beta/\nu^2$, where α and β are constants, and the term $(4\pi/c)^2$ has been absorbed into α. In section 3 it will be shown that setting β equal to unity gives good agreement, as might be expected because the slope variance is proportional to windspeed, and the value of α which gives best fit with measurements of rough ocean brightness temperature also happens to be close to unity.

Bragg scattering can also be an important process for other surfaces, but here we do not usually have a parameter equivalent to windspeed for the ocean to use in a parameterisation. The value of σ^2 which gave best agreement with aircraft brightness temperature measurements in the mean sense was derived[16,17].

2.3 Multiple-layering

Surfaces often have a fractional coverage by another optically thick medium (e.g. foam on ocean). We therefore multiply the modified reflectivities by (1-F), where F is the fractional coverage of the upper medium[25]. This very simple treatment only works when the upper layer is optically thick and assumed to be black, and is included primarily to solve the foam problem. The effect of vegetation could be parameterised in this way, but has not been in this paper, primarily because of difficulties with representing shadowing effects at large nadir incidence angle.

2.4 Geometric roughness

Roughness which has a large scale compared to the wavelength of observation gives geometric specular reflection. Large scale roughness effects are not modelled except for the ocean surface. To calculate ocean emissivity it is necessary to have a model of wave slopes as a function of windspeed[26]. A geometric calculation is required to calculate the contribution from each slope measured by a radiometer. Furthermore it is necessary to know the previous path of the reflected ray from each slope, and to know which have undergone previous reflections on other slopes. Therefore it is computationally very expensive. Its accuracy depends on how representative the ocean slope model is. Large scale roughness often corresponds to ocean swell, which may have no relation to instantaneous windspeed, especially at low instantaneous windspeed. This model is parameterised in terms of windspeed, although flexibility remains separately to parameterise instantaneously induced roughness from the background windspeed and ocean swell roughness directly from a wave model. In this model the specular reflectivities have a factor $\Delta R_v(\nu,\theta,U)$ and $\Delta R_h(\nu,\theta,U)$ added to vertical and horizontal polarisations respectively, where U is windspeed to account for geometric roughness effects. This follows the approach of Petty and Katsaros[27], except that all the differences between a specular reflection and an integration across all the slopes, are

included in $\Delta R_v(\nu,\theta,U)$ and $\Delta R_h(\nu,\theta,U)$. ΔR_v and ΔR_h are parameterised in terms of windspeed, frequency and the secant of view angle. This scheme builds on that proposed by Petty and Katsaros except that more predictors are used to calculate ΔR_h and ΔR_v, and no predictor using skin temperature is employed (it was found to be unnecessary). At a surface skin temperature of 273K and assuming the variance of roughness to be proportional to windspeed the Petty and Katsaros formula reduces to

$$\Delta R \propto U(a+b.\theta), \tag{5}$$

where a and b are coefficients which depend on frequency and polarisation. In this model the secant of the view angle is found to be a better predictor than angle and the polynomial is extended to achieve higher accuracy (~0.1-0.3%) such that

$$\Delta R \propto U(a+b.\sec\{\theta\})+c.\sec\{\theta\}+d.\sec^2\{\theta\}+e.U^2, \tag{6}$$

and a, b, c, d and e are coefficients which are a function of frequency and polarisation. Furthermore in this model it is found that a, b, c, d and e are all monotonic functions of frequency, ν, such that $a=a_0+a_1\cdot\nu$ and similarly for b, c, d and e.

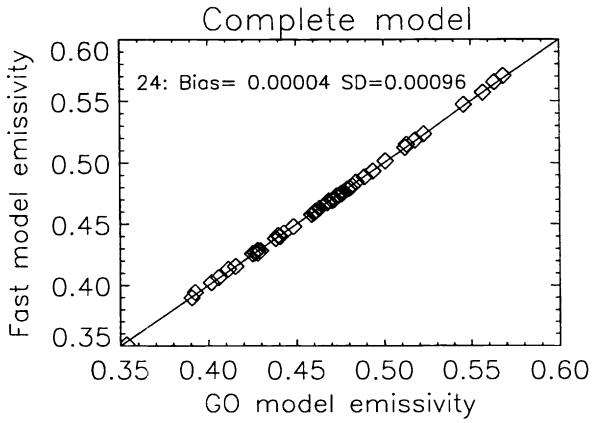

Figure 1: The fit of the fast model to the full geometric optics (GO) model at 24 GHz, for windspeed 0-12 ms^{-1}, skin temperature 0-25°C and incidence angle 0-45°.

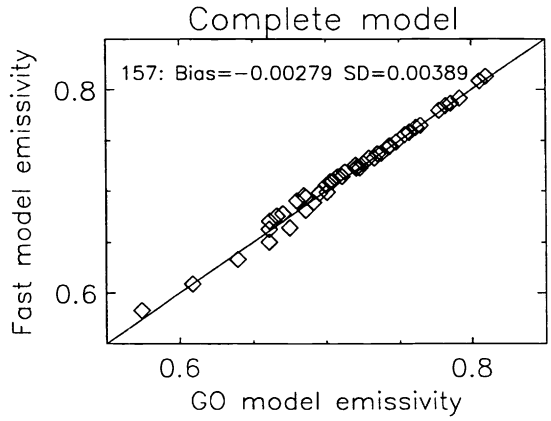

Figure 2: The fit of the fast model to the full geometric optics (GO) model at 157 GHz for the same range of conditions as Fig. 1.

In this model ΔR is defined to include reflected rays from non-specular angles, so no additional non-specular term is needed. Mathematically ΔR is defined as

$$\Delta R=(T_s-T\uparrow)/(T_s-T\downarrow)-R, \tag{7}$$

where the surface brightness temperature, $T\uparrow$, is calculated making as few simplifying assumptions as possible, T_s is skin temperature and $T\downarrow$ is sky brightness temperature. In their paper Cox and Munk[26] presented two slope variances, without and without an oil-slick. The slick data is assumed to correspond to ocean roughness where small scales have been suppressed. At high frequency the total Cox and Munk[26] geometric slope roughness is used (i.e. the non-slick roughnesss), and for frequencies below 35 GHz the slope variance is linearly reduced towards the Cox and Munk slick value at 0 GHz[25,28]. Fig. 1 compares the fast model to the full geometric optics solution for 24 GHz, and Fig. 2 shows the same result at 157 GHz. At low frequency the fast model is near perfect, the standard deviation being less than 0.001 with no bias. At higher frequency the fit is slightly less good, with a standard deviation just over 0.003. This is because the geometric slope variance is higher and the correction due to roughness is correspondingly larger. The loss of accuracy in the fast model is still small compared to the uncertainty in the geometric optics model, which is around 0.01, and is also larger at higher frequency.

2.5 Depolarisation

The four processes modelled above do not and cannot allow for all mechanisms which depolarise the emitted radiance. Importantly biomass depolarises, and other surfaces such as sea-ice show less polarisation than would be expected from a specular reflectivity calculation. If good agreement with the specular calculation is found for nadir observations the depolarisation can not be caused by geometric roughness, which would decrease the nadir reflectivity. Therefore to allow the model to fit aircraft observations a fifth term, simply called a depolarisation factor, Q(n), is added[16,17]. Depolarisation is a function of roughness, and so it may be possible to parameterise Q as a function of σ, but this has not been attempted.

2.6 The complete model

Dropping the arguments, the emissivity forward model can be written

$$E_v=(1-\{(1-F)(R_v.B+\Delta R_v\})Q+(1-\{(1-F)(R_h.B+\Delta R_h\})(1-Q)$$

and

$$E_h=(1-\{(1-F)(R_h.B+\Delta R_h\})Q+(1-\{(1-F)(R_v.B+\Delta R_v\})(1-Q). \tag{8}$$

Surface type	Permittivity coefficients			Roughness	Depolarisation
	ε_s	ε_∞	ν_r GHz	σ mm	Q
OPEN WATER					
Ocean	From Lamkaouchi (1997)			0.1U	0.0
SEA ICE					
Grease ice	23.7	7.7	17.3	0.0	0.15
Baltic Nilas	1.6	3.3	2.2	0.0	0.0
New ice (no snow)	2.9	3.4	27.0	0.0	0.0
New ice (snow)	2.2	3.7	122.0	0.0	0.15
Brash ice	3.0	5.5	183.0	0.0	0.0
Compact pack ice	2.0	17×10^5	49×10^6	0.0	0.0
Fast ice	1.5	77.8	703	0.1	0.35
Lake ice + snow	1.8	67.1	534	0.1	0.15
Multi-year ice	1.5	85×10^3	47×10^5	0.0	0.0
WINTER LAND SURFACES					
Forest and snow	2.9	3.4	27.0	0.0	0.0
Deep dry snow	3.0	24.0	60.0	0.1	0.15
Frozen soil	117.8	2.0	0.19	0.2	0.35
SUMMER LAND SURFACES					
Forest	1.7	1.0	163.0	0.0	0.5
Open grass	2.2	1.3	138.0	0.0	0.42
Bare soil	2.3	1.9	21.8	0.0	0.5

Table 1: Emissivity model coefficients from[10, 16, 17]. Note for ocean σ=0.1U where U=10m windspeed.

The parameter F is neglected for surfaces other than foam-covered water, and ΔR_v and ΔR_h are also only calculated for the ocean. The coefficients ε_s, ε_∞, ν_r, σ and Q are listed in Table 1 for a range of surfaces. Note for some surfaces small scale roughness has been absorbed in to ε_s, ε_∞ and ν_r, and σ is set to zero.

3. VALIDATION

Fig. 3 shows the calculated emissivity plotted against values estimated from measurements of ocean brightness temperatures made by the radiometers cited in the introduction. The "observed" emissivity has an accuracy of about 0.005 at 24 GHz and 0.01 at 157 GHz. Four validation plots are shown: the "complete" model, the complete model with no representation of geometric roughness, the complete model with no representation of Bragg scattering and finally the model with no treatment of geometric roughness or Bragg scattering. At 24 GHz the standard deviation of the fit falls from 0.0154 when roughness is not modelled to 0.0105 when roughness is modelled. The most significant part of this improvement arises from modelling geometric roughness, but the Bragg component is also important. Bias is similarly reduced from 0.0192 to 0.0035, indicating that a large part of both the geometric and Bragg effects is one-sided (i.e. bias). Results are slightly different at 157 GHz and are shown in Fig. 4. Again modelling roughness improves the fit from a standard deviation of 0.0204 to 0.0130, but almost all of this arises from geometric roughness, the Bragg component being unimportant at high frequency.

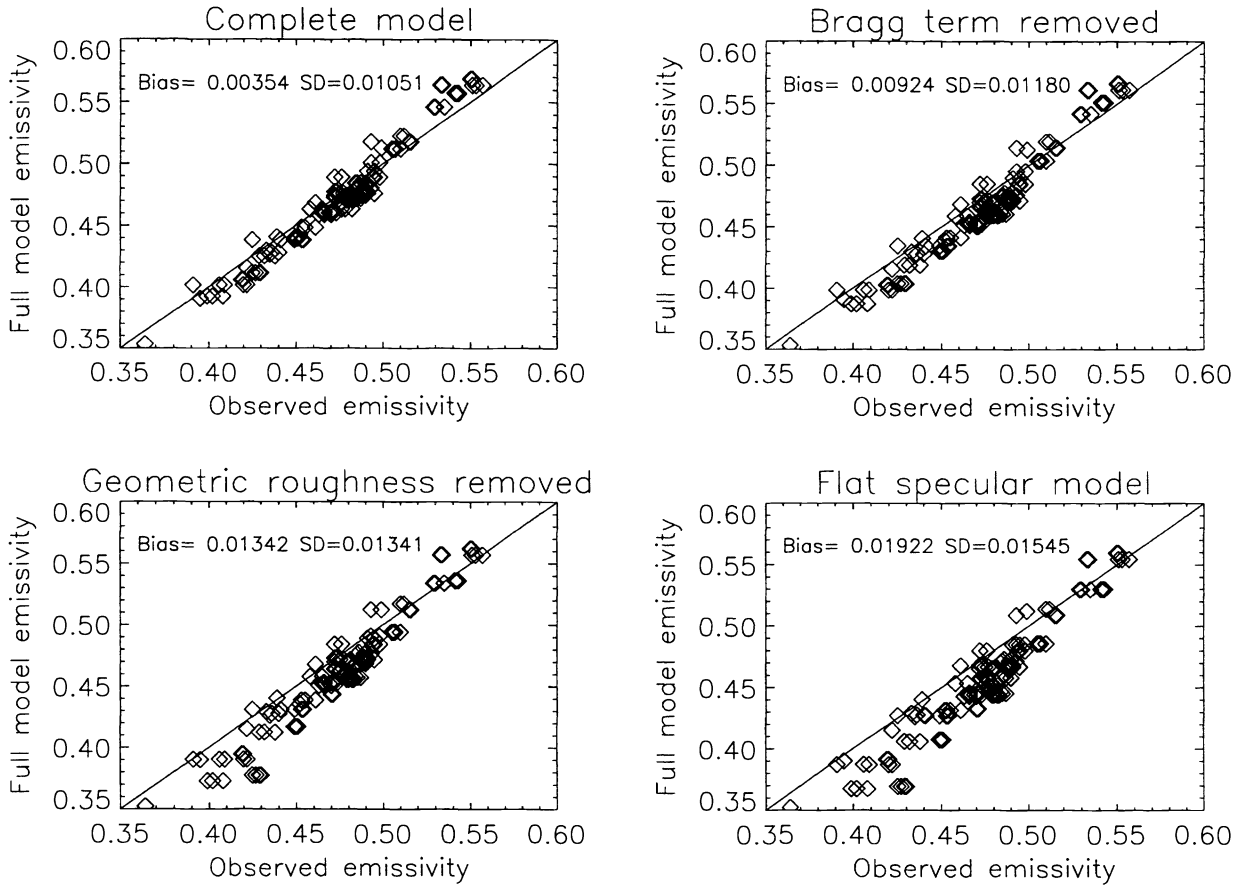

Figure 3: Calculated emissivity from full model versus emissivities estimated from airborne radiance measurements at 24 GHz. The comparison is shown using a specular flat model (with foam), a model with no Bragg term, a model with no geometric optics integration and finally the full model. The roughness modelling is realistic in the sense that it improves the fit to the observation both in terms of bias and standard deviation.

Fig. 5 shows validation versus view angle and for vertical and horizontal polarisations for both a calm ocean surface (windspeed 0 ms^{-1}) and a rough ocean surface (windspeed 12 ms^{-1}) at 24 GHz. Without the modelling of roughness a significantly higher bias occurs at high windspeed, whereas the complete model gives a residual bias of +1% near nadir and +1.5% (horizontal polarisation) and -1.5% (vertical polarisation) at 40° for the calm and rough ocean cases. Fig. 6 shows a plot of emissivity differences (observed minus calculated), again at 24 GHz, against windspeed at the nadir view angle. When roughness is not modelled a linearly increasing bias with windspeed is observed, which is removed by the modelling of roughness (note both flat and rough models accounted for the effect of whitecapping).

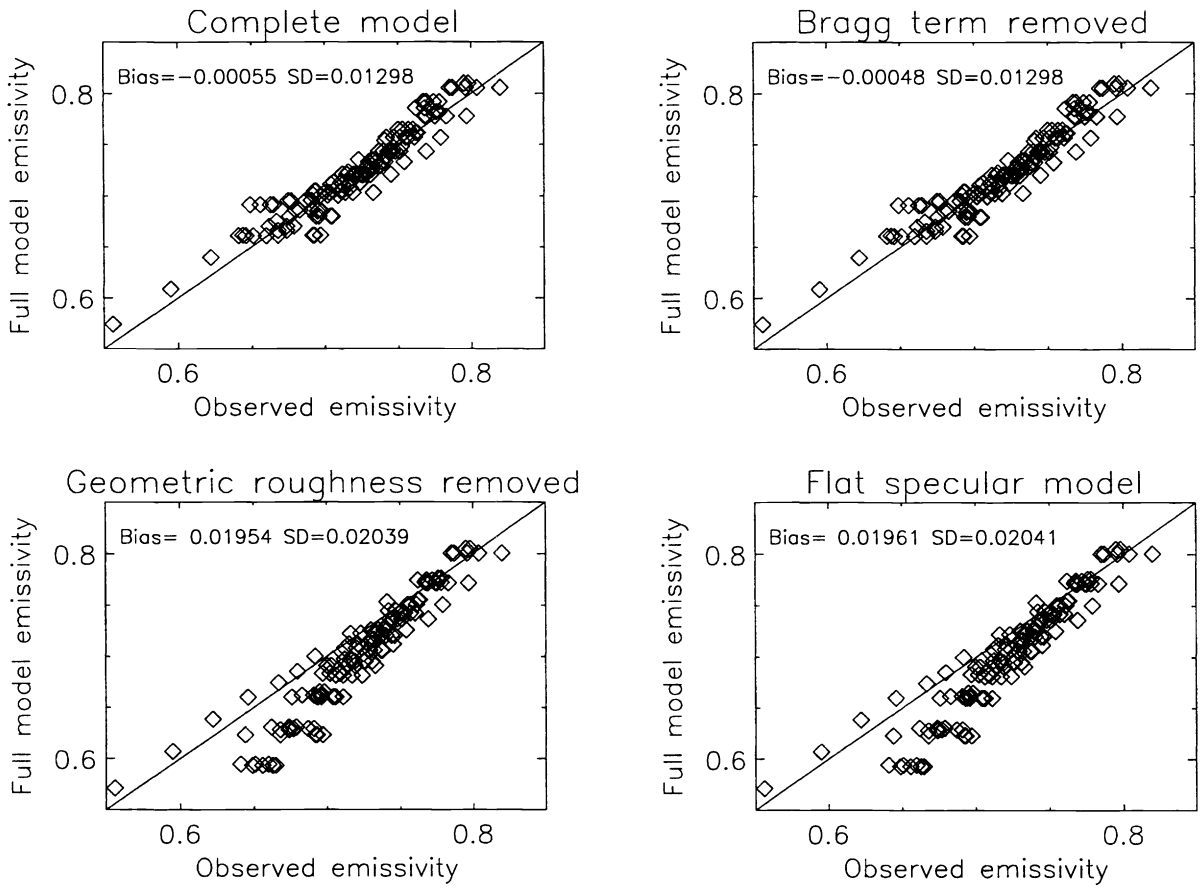

Figure 4: As Fig. 3 for 157 GHz.

For other surfaces validation is more difficult. It is not straightforward to separate emissivity model errors from the errors due to inadequate surface parameter information. For example dense forest has a highly predictable emissivity which varies little with snow cover and wetness. However more open forest has a variable emissivity, because of variations in emissivity arising from the forest floor. Therefore the emissivity model really needs to know the fractional coverage of forest in the field of view. Typically this will not be known. However it is important to clarify that this is a surface parameter error not an emissivity model error, and an improved estimate of the true value of fractional coverage can potentially be retrieved from the radiances. Emissivity model errors arise when the physics in the model is incorrect, or empirically tuned coefficients are not globally representative. Assumptions such as specular reflection, Bragg term coefficients, effective permittivities, depolarisation all have errors which contribute to the forward model error. Because we have simplified the model to be consistent with the quality of surface parameter information available, the forward model error for non-sea surfaces will usually be higher than for sea surface. If the emissivity model error is high, this may be a limiting factor in the usefulness of the observations, and cannot be reduced by improved estimates of the quantities used by the models. Much larger gross errors can occur if the wrong surface is assumed, but these should be identified by adequate quality control. If two surfaces are radiometrically very similar, the emissivity model coefficients will be adequate as a first guess for either surface when retrieving atmospheric profiles. A number of existing studies have derived emissivities for a wide range of surface types at frequencies above 20 GHz[9,11,13,15,29]. Comparison of the current model with these studies shows agreement is usually within a few percent, as illustrated by Fig. 7 (mean emissivity) and Fig. 8 (polarisation difference). Difficulties do arise where surface type classifications are poorly defined ("dense" forest, "dry" snow, "young or new" ice etc.), and these can cause larger differences.

Figure 5: Difference between calculated emissivity and "observed" emissivity at 24 GHz versus incidence angle for vertical and horizontal polarisations. In each figure there are two pairs of curves. The upper pair is for the rough ocean

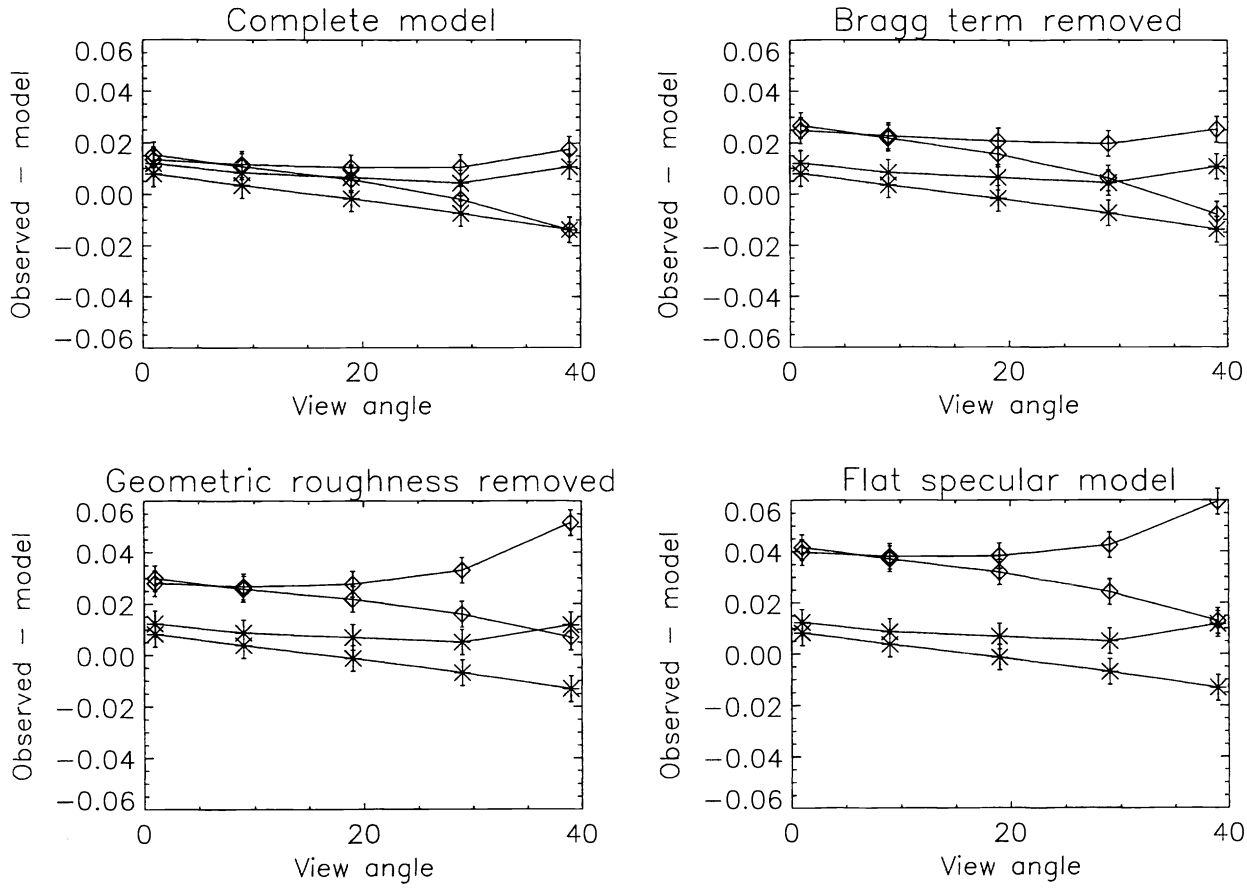

Figure 5: Difference between calculated emissivity and "observed" emissivity at 24 GHz versus incidence angle for vertical and horizontal polarisations. In each figure there are two pairs of curves. The upper pair is for the rough ocean (wind-speed 12 ms^{-1}) and the lower pair for a calm ocean. In each pair the upper curve is horizontal polarisation (i.e. at large view angle the model tends to underestimate horizontal polarisaion and overestimate vertical polarisation so more depolarisation is occuring than would be expected). This could be corrected by setting Q=0.03 for the ocean surface.

For land surfaces the emissivity depends strongly on vegetation cover. The model of Isaacs *et al.*[11] and the study by Prigent *et al.*[9] all showed emissivity to rise with increasing vegetation biomass, especially for horizontal polarisation. However the values vary considerably, partly due to varying definitions of land surface classes. For example bare soil 85-90 GHz mean emissivity (the average of vertical and horizontal) ranges from as low as 0.89 and 0.92 in the studies by Prigent *et al.* and Mätzler[15] to 0.96 in this paper and 0.98 in Felde and Pickle[13]. Those studies which separated frozen soil from unfrozen soil showed emissivity to increase by around 0.02 on freezing. Short grass very slightly increases the emissivity (increases range from 0.00 to 0.02), but forest or dense vegetation increases the emissivity close to unity (with the exception of Felde and Pickle, which showed a lower emissivity for dense forest than soil). Snow cover also significantly changes the emissivity. The study by Mätzler is the most comprehensive for frequencies above 20 GHz. This study showed the emissivity of dry snow to be low (0.6-0.8) and most variable at highest frequency, in agreement with Hewison's results[16,17]. The low emissivity is due to volume scattering in the snow crust, which increases with decreasing wavelength. The precise depression of the brightness temperature depends on the thickness of any refrozen crust and the depth of dry "powder" snow, which is variable and gives the observed high variability in emissivity. This noise, which occurs over short horizontal distances, will be spatially averaged over a satellite instrument field of view. The radiative transfer is almost linear, so the effective emissivity will have a mean close to the mean which would be expected from the mean crust/dry snow thickness in the field of view and have low noise due to the spatial averaging. The model coefficients in Table 1 do not agree with the permittivity model in Mätzler (1994), nor should they be expected to. The fast model coefficients should not be interpreted as Debye parameters and do not correspond to permittivity of real snow, because the effect of scattering has been absorbed into the effective permittivity. For a scattering surface the parameters used in this model have no physical meaning, but the analogy with a Debye form is a convenient mathematical framework.

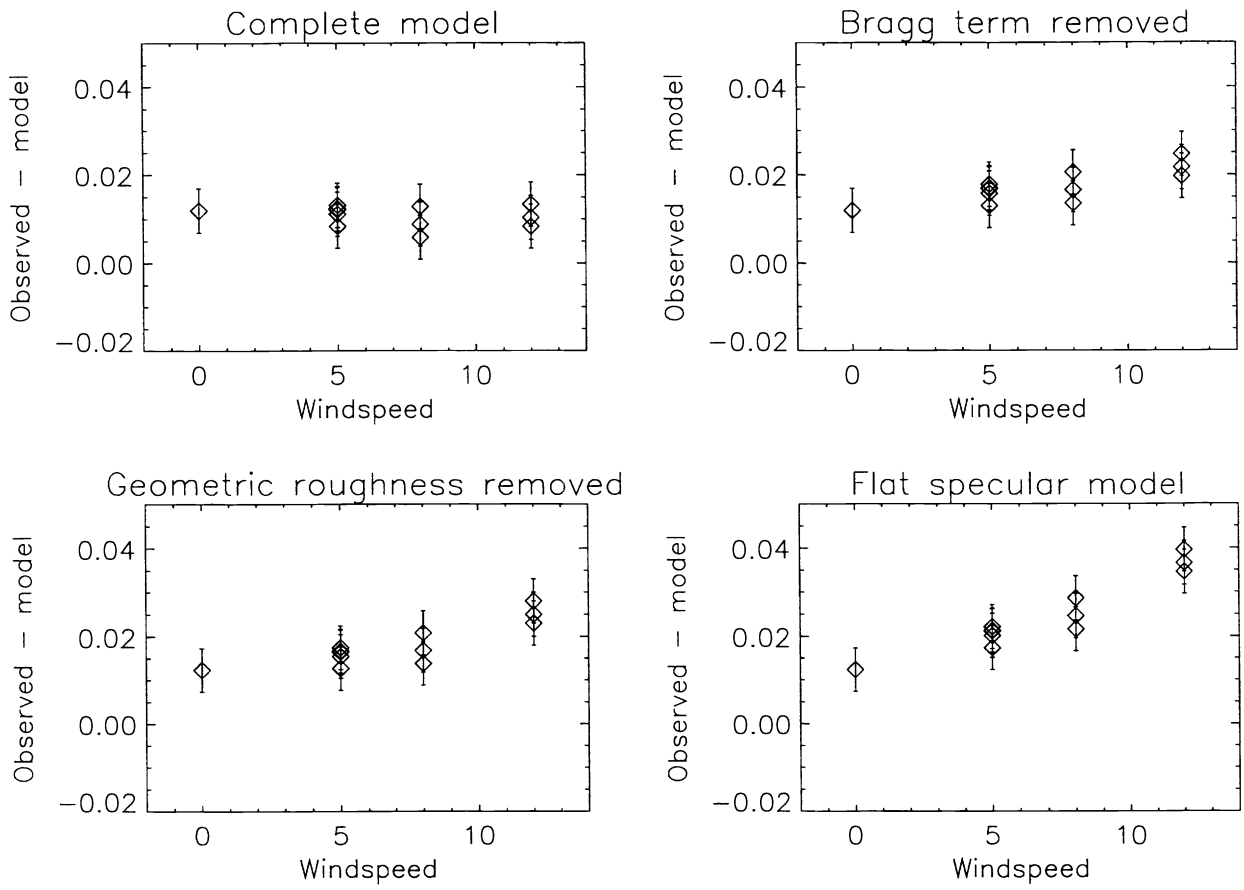

Figure 6. Difference between calculated emissivity and "observed" emissivity at 24 GHz versus windspeed. The linear trend of difference with windspeed for a specular surface is replaced by a constant bias when roughness is modelled.

The results for sea ice have been compared with Comiso *et al.*[29]. Comparing at 90 GHz, the emissivities for open water are in good agreement. The emissivity of nilas is slightly lower in Comiso's study (0.89-0.90, compared with 0.92), probably due to higher salinity in the Weddell sea ice compared to the Baltic. The grease ice emissivity from Comiso is lower than from Hewison, but Comiso's open water emissivity is also lower by the same amount, implying the precise emissivity of grease ice depends strongly on the sea state. This would be expected, because grease ice does not suppress ocean roughness. Comiso's young ice category is assumed to be equivalent to Hewison and English's[16] bare new ice, in which case Comiso again found a lower emissivity (0.86 against 0.91). Compact pack ice in Hewison and English gives a very similar emissivity to Comiso's smooth and rough first year sea ice, both around 0.85. Therefore the two studies give reasonable agreement for very thin ice and older, snow-covered ice, but the model presented in this paper may be biased towards low salinity ice for young, snow-free ice types. Hewison and English confirmed that signatures usually associated with first-year or multi-year sea ice can be observed in much younger snow-covered compact pack ice, fast ice and lake ice. Comiso's young ice does not have the large polarisation difference predicted for new ice. The new ice was one-two days old, thin and snow-free. Comiso's result shows that increasing roughness and partial snow-cover rapidly depolarise the emission from the thin ice layer, and the new ice model is only suitable for ice which has undergone no deformation.

4. CONCLUSIONS

A fast emissivity model has been generated from a mixture of theoretical and empirical information, and building on existing studies where possible. It has been demonstrated to give good agreement with aircraft observations of emissivity, and to give similar emissivities to previous studies where classifications are consistent. A new parameterisation of

geometric roughness (for the ocean surface) and Bragg scattering has been used, which lends itself to fast computation and simple calculation of model tangent-linear and adjoint, whilst retaining a fully generic capability. For the ocean surface the model is accurate to 0.5%. For other surfaces the accuracy is variable, ranging from 5-10% for snow surfaces, 2-5% for ice and open land and 1-2% for forest. Comparison of existing measurements and model predictions has been attempted for a range of surfaces but is hampered by varying or imprecise definitions of surface categories, and lack of information on heterogeneity. Nonetheless for most surface categories fair agreement can be achieved. The model is designed for atmospheric sounding applications. It does not have the sophistication to retrieve surface parameters except for the ocean, but is intended to solve the boundary condition problem in retrieving water vapour, temperature, cloud liquid water and precipitation rate from passive microwave radiometers.

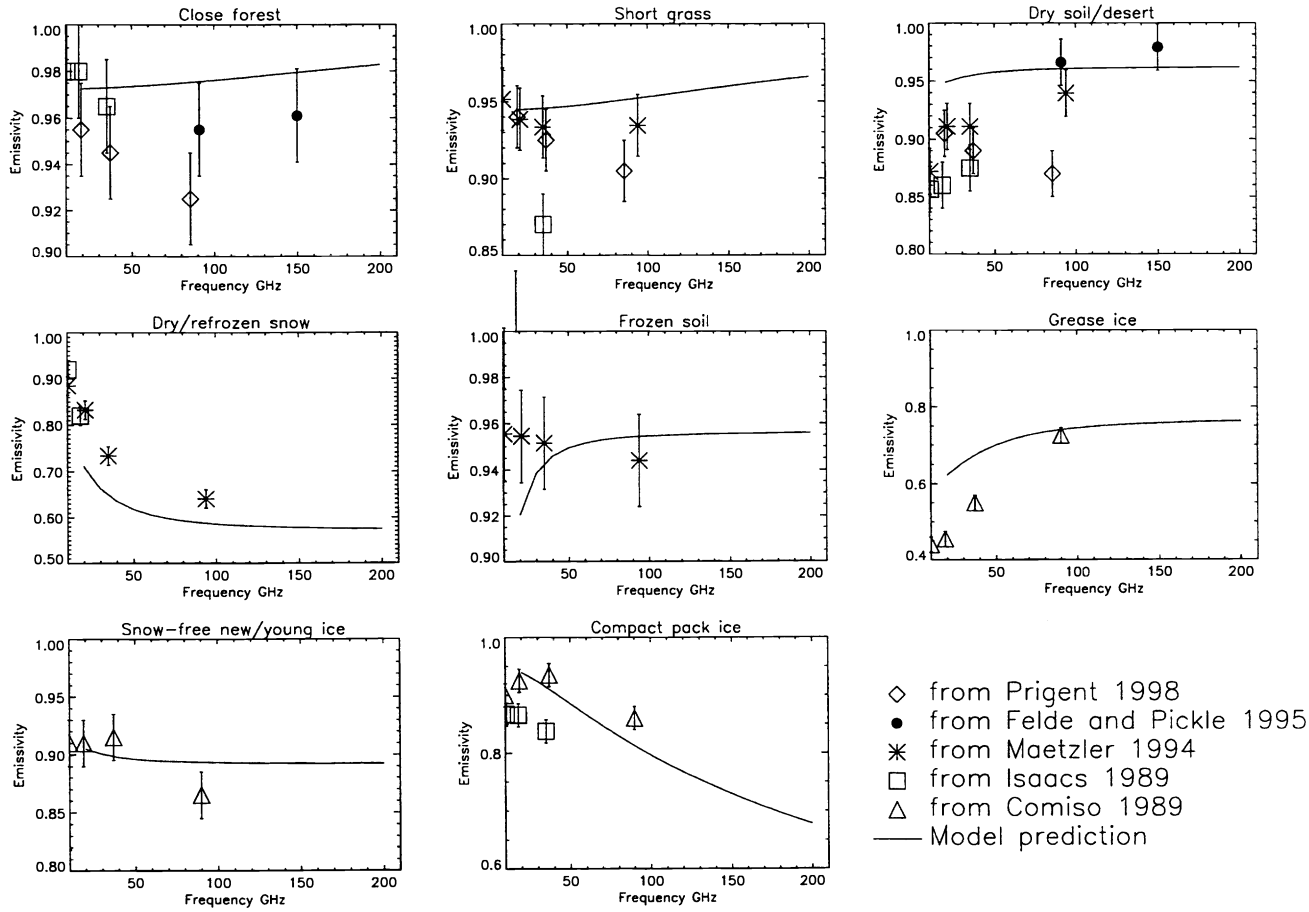

Figure 7. Mean emissivity (vertical plus horizontal polarisation) plotted against frequency from the fast model and from a range of literature sources for land surface types (soil/desert, frozen soil, grass, forest, dry snow) and sea ice (grease ice, bare young ice/new ice, compact pack ice/first year ice). These are for a range of angles 0-54°.

5. ACKNOWLEDGEMENTS

All those who contributed to the success of the airborne radiometer experiments are thanked, and we are grateful to D.C. Jones, J. K. Ridley and J.R. Eyre for comments on the text. Kris Foster processed some of the airborne radiometer data.

6. REFERENCES

1. J.R. Eyre, G.A. Kelly, A.P. McNally, E. Andersson and A. Persson, 1993: Assimilation of TOVS radiances through one dimensional variational analysis., Q. J. Royal Meteorol. Soc., **119**(514), 1427-1463.
2. A.J. Gadd, B.R. Barwell, S.J. Cox and R.J. Renshaw, 1995: Global processing of satellite sounding radiances in a numerical weather prediction system., Q. J. Royal Meteorol. Soc. **121**, 615-630.

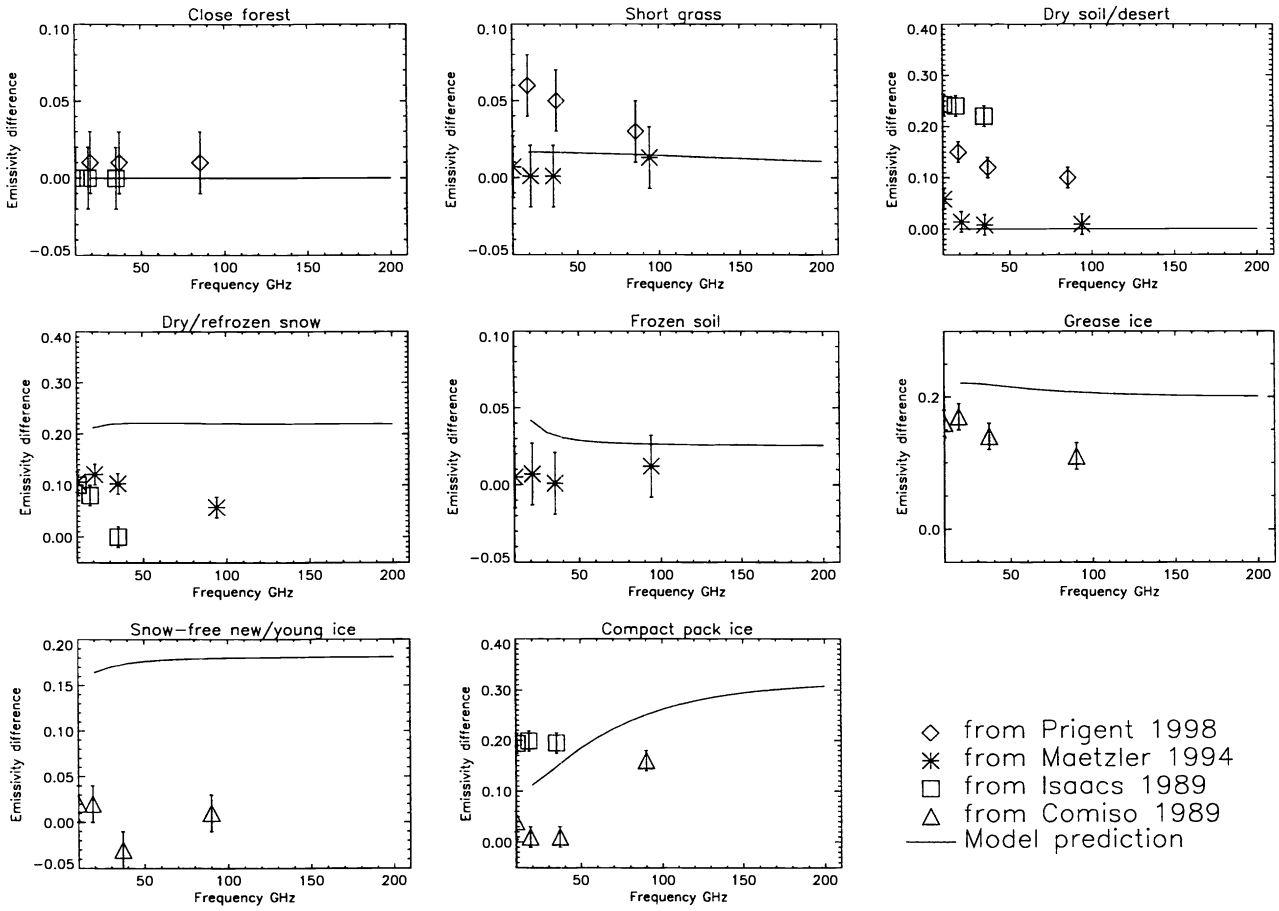

Figure 8. As Fig. 7 but for polarisation difference (vertical minus horizontal) at an incidence angle of 50-53^{o}.

3. J.C. Derber and Wan-Shu Wu, 1997: The use of TOVS radiances at NCEP. Tech. Proc. 9th International TOVS Study Conference; Igls, Austria; 20-26 February 1997; Ed.: J.R. Eyre; Published by ECMWF, Reading, UK; pp. 103-112.
4. A.S. Jones and T.H. Vonder Haar, 1990: Passive microwave remote sensing of cloud liquid water over land regions. J. Geophys. Res., **95**, 16673-16683.
5. A.S. Jones and T.H. Vonder Haar, 1997: Retrieval of microwave surface emittance over land using coincident microwave and infrared satellite measurements., J. Geophys. Res., **102**, 13609-13626.
6. T.J. Greenwald, C.L. Combs, A.S. Jones, D.L. Randel and T.H. Vonder Haar, 1997: Further developements in estimating cloud liquid water over land using microwave and infrared satellite measurements. J. Appl. Meteorol., 36, 389-405.
7. C.L. Combs, T.J. Greenwald, A.S. Jones, D.L. Randel and T.H. Vonder Haar, 1998: Satellite detection of cloud liquid water over land using polarization at 85.5 GHz.., Geophys. Res. Letters, **25**, 75-78
8. C. Prigent and R. Rossow, 1998: Retrieval of surface and atmospheric parameters over land from SSM/I: potential and limitations., *Submitted to J. Geophys. Res.*

9. C. Prigent, E. Mathews and R. Rossow., 1997: Microwave land surface emissivities estimated from SSM/I observations. J. Geophys. Res., **102**, 21867-21890.
10. S.J. English, 1998: Estimation of temperature and humidity profile information from microwave radiances over different surface types. *To be submitted to J. Appl. Meteorol.*
11. R.G. Isaacs, Ya-Qui Jin, R.D. Worsham, G. Deblonde, V.J. Falcone, 1989: The RADTRAN microwave surface emission models., IEEE Trans. Geoscience and Remote Sensing, **27**(4), 433-440.
12. A.A. Van de Griend and M. Owe,1994: Microwave Vegetation Optical Depth and Inverse Modelling of Soil Emissivity Using Nimbus/SMMR Satellite Observations, Meteorol. Atmos. Phys., **54**, 225-239.
13. G.W. Felde and J.D. Pickle, 1995: Retrieval of 91 and 150 GHz Earth surface emissivities., J. Geophys. Res. 100(10), 20855-20866.
14. I. Sherjal, M. Fily, O. Grosjean, J. Lemorton, B. Lesaffre, Y. Page and M. Gay,1998: Microwave Remote Sensing of Snow from a Cable Car at Chomonix in the French Alps., IEEE Trans. Geosci. Remote Sens., **36**(1), 324-328.
15. C. Mätzler, 1994: Passive microwave landscapes in winter., Meteorol. and Atmos. Phys. **54**, 241-260.
16. T.J. Hewison and S.J. English, 1998: Results of a microwave airborne campaign over snow and ice., *submitted to IEEE Transactions on Geophys and Remote Sensing.*
17. T.J. Hewison, 1998: Airborne measurements of NOPEX land surface emissivity at millimetre wavelengths., *submitted to IEEE Transations on Geophys. and Remote Sensing.*
18. S. Surdyk and M. Fily, 1995: Results of a stratified snow emissivity model plus modelling efforts based on the wave approach: application to the Antarctic ice sheets., J. Geophys. Res., **100**(C5), 8837-8848.
19. J.C. Maxwell-Garnett, 1904: Colours in metal glasses and metallic films., Phil. Trans. Roy. Soc., A203, 385-420.
20. N.C. Grody, 1993: Remote sensing of the atmosphere from satellites using microwave radiometry.; Chapter 6 of A tmospheric Remote Sensing by Microwave Radiometry; Ed.: M.A. Janssen; John Wiley and Sons, In.
21. K. Lamkaouchi, A. Balana and W.J. Ellison, 1997: New permittivity data for sea water (30-100 GHz). Extension of ESA report 11197/94/NL/CN.
22. S.T. Wu and A.K. Fung, 1972: A noncoherent model for microwave emissions and backscattering from the sea surface., J. Geophys. Res., **77**, 5917-5929.
23. B.J. Choudbury, T.J. Schmugge, A. Chang and R.N. Newton, 1979: Effect of surface roughness on the microwave emission from soils., J. Geophys. Res., **84**(C9), 5699-5706.
24. J.R. Apel., 1994: An improved model of the ocean surface wave vector spectrum and its effect on radar backscatter., J. Geophys. Res., **99**(C8), 16269-16291.
25. T.T. Wilheit, 1979: A model for the microwave emissivity of the ocean's surface as a function of wind speed., IEEE Transactions on Geoscience Electronics, **GE-17**, 244-249.
26. C. Cox and W. Munk, 1955: Some problems in optical oceanography., J. Marine Res., **14**, 63-78.
27. G.W. Petty and K.B. Katsaros, 1994: The response of the SSM/I to the marine environment. Part II. A parameterization of the effect of the sea surface slope distribution on emission an reflection., J. Atmos. and Oceanic Tech., **11**(3), 617-628.
28. F. Wentz, 1983: A model function for ocean microwave brightness temperatures., J. Geophys. Res., **88**(C3), 1892 -1908.
29. J.C. Comiso, T.C. Grenfell, D.L. Bell, M.A. Lange, and S.F. Ackley, 1989: Passive microwave in situ observations of winter Weddell sea ice., J. Geophys. Res., **94**(C8), 10891-10905.

For further information -
SJE (corresponding author): Email: senglish@meto.gov.uk; WWW: http://www.meto.gov.uk/sec5/NWP/SSG.html; Telephone +44 1344 854652l; Fax +44 1344 854026. TJH: Email: tjhewison@meto.gov.uk; Telephone +44 1252 595781